Ionization Energy of *p*-Fluoroaniline and Vibrational Levels of *p*-Fluoroaniline Cation Determined by Mass-Analyzed Threshold Ionization Spectroscopy

W. B. Tzeng* and J. L. Lin

Institute of Atomic and Molecular Sciences, Academia Sinica, P.O. Box 23-166, #1 Section 4, Roosevelt Road, Taipei 106, Taiwan, Republic of China

Received: June 21, 1999; In Final Form: August 9, 1999

Mass-analyzed threshold ionization (MATI) and two-color resonant two-photon ionization (2C-R2PI) methods were used for detailed studies of the adiabatic ionization energy of *p*-fluoroaniline (PFA) and the vibrations of this molecule in the cationic ground state. The threshold ion spectra were recorded for PFA via the 0° vibrationless and the $6a^1$, 1^1, 12^1, $6a^1l^1$, and $6a^112^1$ vibrational levels of the S_1 state. The adiabatic ionization energy of PFA is found to be 62 543 ± 4 cm^{-1} by the MATI spectroscopy and 62 550 ± 7 cm^{-1} by the 2C-R2PI spectroscopy. Results show that the active modes are mostly related to in-plane ring vibrations of the ion. All of these experimental data are presented for the first time. Ab initio and density functional theory calculations were also performed for predicting the ionization energy and vibrational frequencies. Comparative studies show that the measured and calculated results are in very good agreement.

1. Introduction

Recording spectra of molecular ions is often a nontrivial task using conventional spectroscopic techniques. Recent advances in the spectroscopy of ions have focused on the development of zero-kinetic energy (ZEKE) photoelectron spectroscopy.[1−3] This method involves the excitation of long-lived high Rydberg states and their subsequent ionization in a delayed pulsed electric field, leading to production of threshold ions in well-defined energy states. This high-resolution spectroscopic technique can provide a precise determination on the ionization threshold of molecules as well as vibrational levels of ions. Since ZEKE technique is subject to the detection of electrons, it has no mass information. In a similar approach, mass-analyzed threshold ionization (MATI) method involves detection of ions rather than electrons and thus can provide an unambiguous mass resolved spectral information.[4−8] These methods have been adopted in the spectroscopic and dynamic studies of molecules, van der Waals complexes, and clusters. Recently, threshold ion-pair production spectroscopy (TIPPS) which is conceptually analogous to the ZEKE and MATI methods has been developed for the determination of bond dissociation energy of HCl in an accuracy as high as 0.8 cm^{-1}.[9]

Aniline and its derivatives are of great industrial importance, particularly in the pharmaceutical and chemical industries. To the best of our knowledge, experimental data on the ionization energy and many properties of substituted anilines in the ionic state are rare in the literature. *p*-Fluoroaniline (PFA) can serve as a model system for studying the substitution effects on chemical properties of aromatic molecules, because the F atom withdraws electrons from the ring whereas the NH_2 group donates its lone pair electrons to the ring. Previous investigations on PFA have focused on the electronic and vibrational properties in the ground and excited states. Microwave[10] studies showed that PFA in the S_0 state is nonplanar with a pyramidal configuration for the NH_2 part. The angle between the phenyl ring and the NH_2 planes was determined to be 46°. Thus, PFA belongs to the C_s point group. Rotational band contour analysis[11] suggested that in the S_1 state this molecule becomes planar with C_{2v}, symmetry and contracts along the axis containing the N, C_1, C_4, and F atoms. The corroborating measurements on dipole moments[12] suggested that PFA in the S_1 state has a quinoid-like resonance structure. The results of ab initio calculations are found to be in good agreement with those of experiments.[13,14]

The ground state vibrations of PFA have been studied using IR[15] and far-IR[16] spectroscopy. The UV absorption spectrum of this molecule near the $S_1 \leftarrow S_0$ transitions has been reported.[17] Furthermore, the $S_1 \leftarrow S_0$ transition in PFA has been investigated by one-color resonant two-photon ionization (1C-R2PI) spectroscopy.[13,14,18] Results from these studies have increased our knowledge about the structures and vibrations of this molecule in the S_0 and S_1 states. But, little is known about this molecule in the ionic state.

In this paper we report the first determination of the adiabatic ionization energy of PFA and the vibrational levels of the PFA cation by using two-color resonant two-photon ionization (2C-R2PI) and MATI spectroscopy. Ab initio and density functional theory (DFT) calculations were also performed for comparison with the experimental results. It was found that the B3LYP/6-311+G** calculations predicted the ionization energy in an accuracy of about 2.3%. In addition, the vibrational frequencies obtained from the UHF/6-31+G* calculations are in very good agreement with the measured values for the PFA ion. The results from experimental and theoretical approaches help us gain more insights into some ionic properties of PFA.

2. Experimental and Computational Details

2.1. Experimental Section. The major components of the time-of-flight (TOF) mass spectrometer used for these experiments are shown in Figure 1. Detailed description on the vacuum, molecular beam, laser, ion optics, and detection systems has been covered in our previous publications.[19,20] In order to ensure the spatial separation of the Rydberg neutrals from the

* Corresponding author. Fax: (886)2-2362-0200. E-mail: wbt@po.iams.sinica.edu.tw.

10.1021/jp992047g CCC: $18.00
Published on Web 10/07/1999

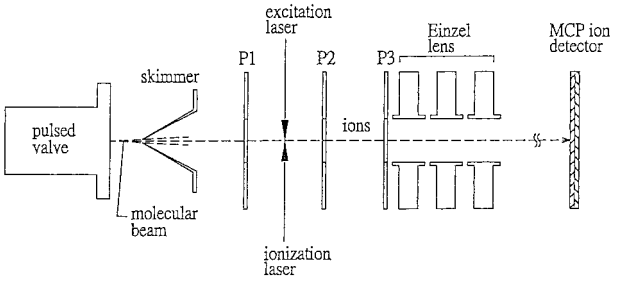

Figure 1. Schematic diagram of TOF mass spectrometer for 2C-R2PI and MATI experiments. See text for experimental details.

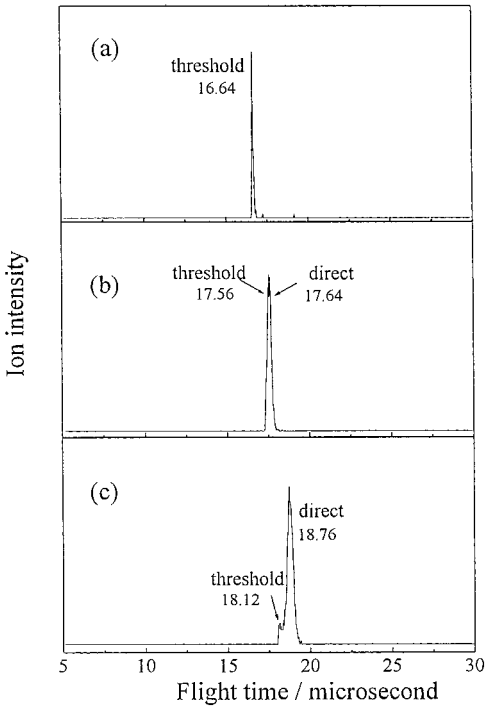

Figure 2. TOF spectra of *p*-fluoroaniline ions obtained at the delay time of the second electric pulse of (a) 8.40, (b) 9.30, and (c) 9.90 μs, respectively.

non-energy-selected prompt ions in the present MATI experiments, the ion optics system was modified as follows. The spacing between plates P1 and P2 became 2.3 cm (region I), whereas that between P2 and P3 remained 1.9 cm (region II). Proper control on the delay time, amplitude, and duration of the two pulsed electric fields allows us to select the pure threshold ions for these experiments, as shown in Figure 2.

The molecular beam was produced by bubbling helium through a reservoir of liquid PFA (Aldrich, 99% purity), that was kept at room temperature. A total pressure (P_0) of 2 bar with ~0.2% PFA was applied behind a pulsed valve (General Valve Corp. Series 9) with 0.15 mm diameter orifice. The pulsed valve was operated at 10 Hz with pulse duration of 80 μs. The molecular beam was collimated by a skimmer located 15 mm downstream from the nozzle orifice. During the experiments, the gas expansion and the ionization regions were maintained at a pressure of 6×10^{-4} and 6×10^{-6} Pa, respectively.

The two color (1+1′) resonant two-photon excitation/ionization process was initiated by utilizing two independent tunable UV laser systems controlled by a pulse delay generator (Stanford Research Systems, DG 535). The first tunable dye laser (Quanta-Ray PDL-3; Rhodamine 610, 640, and Kiton Red dyes) was pumped by a pulsed frequency-doubled Nd:YAG laser (Quanta-Ray GCR-3: 532 nm; repetition rate, 10 Hz; pulse width, 6 ns). The visible radiation was frequency doubled using a wavelength extension system (Quanta-Ray WEX-2) to produce the UV radiation. The UV laser output was focused by a cylindrical lens and directed perpendicularly into the molecular beam. The second tunable UV laser (Lambda-Physik, Scanmate UV with BBO-III crystal; DCM and LDS 698 dyes) was pumped by a frequency-doubled Nd:YAG laser (Quantel, Brilliant B: 532 nm; repetition rate 10 Hz; pulse width, 4 ns). A Fizeau-type wavemeter (New Focus 7711) was used to calibrate the wavelengths of both dye lasers. The respective UV laser outputs were monitored with two separated photodiodes (Hamamatsu 1722S) and fed into a transient digitizer (LeCroy 9450).

The spatial widths of the counterpropagating excitation and ionization UV laser beams were held at about 0.5 mm and 1.5 mm, respectively, in the interaction zone. The excitation laser was fixed to a particular vibronic transition to the S_1, and the ionization laser was scanned from several hundreds wavenumbers above to a few wavenumbers below the adiabatic ionization energy. The intensities of the excitation and ionization laser outputs were adjusted in such a way that the ratio of the two-color to one-color R2PI signals was greater than 50:1. The respective pulse energies of the excitation and ionization lasers were kept at about 80 and 400 μJ, respectively.

In the MATI experiments, both the high-*n* Rydberg neutrals and the non-energy-selected prompt ions were formed simultaneously in the laser and molecular beam interaction zone. Initially, both species traveled with the initial molecular beam velocity towards plate P2. About 50 ns after the occurrence of the laser pulses, a pulsed electric field of −1.0 V/cm (duration = 10 μs) was switched on in region I. Under these conditions, the ions were decelerated but still traveled in same direction as that of the Rydberg neutrals. After a certain time delay (e.g. 8.4 μs), another pulsed electric field of +525 V/cm (duration = 10 μs) was switched on in region II to field-ionize the Rydberg molecules. If this field is switched on before the promptly produced ions reach plate P2, these non-energy-selected direct ions will be rejected. It follows that a pure threshold ion spectrum will be obtained, as shown in Figure 2a. The threshold ions were created by field-ionizing the Rydberg neutrals in region II. The ions were then accelerated and passed a 1.0 m field-free region before being detected by a dual-stacked microchannel plate detector. The ion signal from the detector was collected and analyzed by a multichannel scaler (Stanford Research Systems, SR430). The multichannel scaler and the transient digitizer were interfaced to a personal computer. Mass spectra were accumulated at 1.2 cm^{-1} spacing for 300 laser shots. Composite optical spectra of intensity versus wavelength were then constructed from the individual mass spectra. As the detected ion signal is proportional to the photon intensities of the excitation and ionization lasers for a two-color two-photon process,[21] the obtained optical spectra were normalized to the laser power in order to avoid spurious signals due to shot-to-shot laser fluctuation.

2.2. Computational Section. Ab initio calculations on the ionization energy of PFA and structure and vibrational frequencies of its cation were performed using the GAUSSIAN 94 program package.[22] The unrestricted Hartree−Fock (UHF) procedure using the 6-31+G* basis set was performed for predicting structure parameters and vibrational frequencies of this molecule in the cationic ground state. All calculated vibrational frequencies quoted in this paper were scaled by a factor of 0.95 to approximately correct for the combined errors stemming from basis set incompleteness and negligence of

electron correlation and vibrational anharmonicity. In order to provide a comparison with the measured ionization energy, we have performed the HF, Moller−Plesset (MP) perturbation, and DFT calculations with the optimized structure at the HF/6-31+G* level. The ionization energy was obtained as the difference in total energies of the cation and the corresponding neutral.

3. Results

3.1. TOF spectra. MATI spectroscopy is based on ionization of molecules in the long-lived high Rydberg states. Thus, the separation of threshold ions from the strong background of directly produced ions is crucial for such experiments with energy-selected ions. Neusser and co-workers[23,24] succeeded in two different experimental approaches by using pulsed electric fields in a reflectron TOF mass spectrometer to achieve this task. Here, we demonstrate that the separation of ions formed via threshold and direct ionization processes can also be accomplished by careful setting on the delay time, amplitude, and duration of the pulsed electric fields in regions I and II.

When the wavelengths of the excitation and ionization lasers were tuned to 306.26 nm (32 652 cm^{-1}) and 334.58 nm (29 888 cm^{-1}), respectively, both the high-*n* Rydberg neutrals and the non-energy-selected prompt (direct) ions were formed simultaneously in the interaction region. Figure 2a shows the TOF spectrum of pure threshold ions of PFA at a delay time of 8.40 μs of the second pulsed field (amplitude = +525 V/cm, duration = 10 μs). Under this experimental condition, only the Rydberg neutrals entered region II, whereas the direct ions were rejected. The peak of threshold ion signal has a maximum at 16.64 μs and width of 0.08 μs (fwhm). It is noted that the flight time of the detected threshold ions includes (1) the time for the Rydberg neutrals to travel from the laser−molecular beam interaction zone to plate P2 and (2) the time for the threshold ions to travel from the field ionization region to the ion detector. Thus, the time for the threshold ions to travel from the field ionization region to the ion detector is 8.24 μs.

As the delay time of the second pulsed field increased to 9.30 μs, the peak in the TOF spectrum became broader, as shown in Figure 2b. This indicates that the detected ions originated from both the threshold and direct ionization processes. The peak at 17.56 μs corresponds to the threshold ions, whereas the peak at 17.64 μs corresponds to the direct ions. In principle, high field can enhance the separation of the ionic and neutral species. However, Schlag and co-workers[25] pointed out that the strength of the pulsed field affects the density of the ZEKE states. Since the electric field in region I is also expected to deplete the high-*n* Rydberg species, a small field favors the production of the threshold ions.[26,27] It was found that a pulsed electric field of −1 V/cm in region I not only warranted the separation of the Rydberg neutrals and the direct ions but allowed Rydberg neutrals to survive for being converting to threshold ions in region II.

When the delay time in the second pulsed field increased to 9.90 μs, both Rydberg neutrals and direct ions reached region II. The detected signal contains both the threshold and direct ions, as seen in Figure 2c. A similar observation has been reported in the literature.[28,29] Under this experimental condition, the number of the threshold ions is estimated to be less than 5% of the direct ions. The maximum locations of the signal due to the threshold and direct ions are separated by 0.64 μs. The velocity of the PFA/He seeded beam is measured to be 1400 m s^{-1}, which will be presented in the next section. Therefore, the spatial separation between the Rydberg neutrals and the direct ions is about 0.9 mm, which is consistent with that reported by Grebner and Neusser.[24]

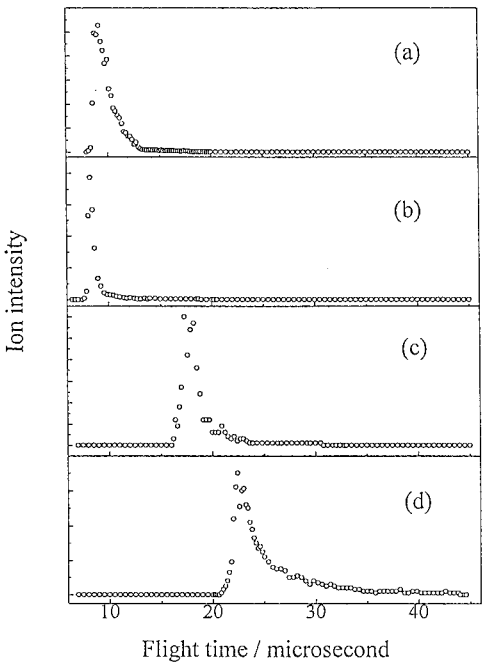

Figure 3. TOF spectra of *p*-fluoroaniline beams with the carrier gas of (a) He at 1.1 bar, (b) He at 2.3 bar, (c) N_2 at 2.3 bar, and (d) Ar at 2.3 bar.

TABLE 1: Characteristics of the *p*-Fluoroaniline Beam

carrier gas (P_0/bar)	v_{mp}/m s^{-1}	$\Delta v/v_{mp}$
He (1.1)	1300	0.17
He (2.3)	1400	0.07
N_2 (2.3)	670	0.08
Ar (2.3)	540	0.08

Since the detected flight time of threshold ions includes the time for Rydberg neutrals to travel from the laser−molecular beam interaction zone to plate P2, the present experimental method can also be used to measure the velocity of the molecular beam containing Rydberg neutrals. This was done by recording the signal of threshold ions as a function of delay time of the pulsed electric field in region II. All other experimental conditions remain the same as those for obtaining Figure 2a. Figure 3a−d shows the TOF spectra of PFA observed in a PFA/He seeded beam at P_0 = 1.1 bar, a PFA/He seeded beam at P_0 = 2.3 bar, a PFA/N_2 seeded beam at P_0 = 2.3 bar, and a PFA/Ar seeded beam at P_0 = 2.3 bar. Since the distance from the laser−molecular beam interaction zone to plate P2 is 1.2 cm, the velocity of the molecular beam can be obtained from the TOF spectrum. The most probable velocities (v_{mp}) and the ratio $\Delta v/v_{mp}$ for these seeded molecular beams determined by the spectra are summarized in Table 1. Here, Δv represents the velocity spread (fwhm) of the beam. It is clear that the lighter carrier gas yields the faster beam. In addition, a higher stagnation pressure in the nozzle gives rise to a fast beam and a small $\Delta v/v_{mp}$. This observation of the characteristics of molecular beams is consistent with those found by using the chopper wheel method and laser hole burning spectroscopy.[30] In order to have a good molecular beam quality, a PFA/He seeded beam at a total stagnation pressure of 2.3 bar was applied for all of the 2C-R2PI and MATI experiments presented in this paper.

3.2. 2C-R2PI Spectrum. Figure 4 shows the 2C-R2PI spectrum of PFA, which was recorded via the vibrationless level 0^0 (32652 cm^{-1}) of the lowest electronically excited S_1 state.

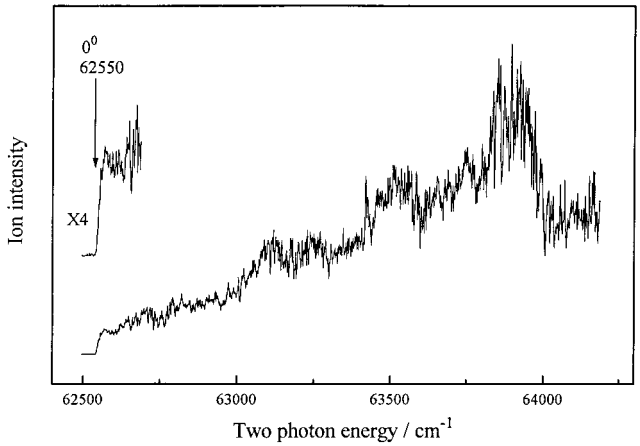

Figure 4. 2C-R2PI spectrum of *p*-fluoroaniline.

TABLE 2: Levels of *p*-Fluoroaniline in the S_1 State, Used as Intermediate States in the MATI Experiments

level	vibrational energy/cm^{-1}
0^0	0
$6a^1$	434
1^1	774
12^1	829
$6a^11^1$	1206
$6a^112^1$	1262

A step which corresponds to the ionization threshold of PFA is clearly seen at a total photon energy of 62 550 ± 7 cm^{-1} (ca. 7.755 eV). This measured value is in good agreement with the estimated value of ≤8.18 eV on the basis of molecular orbital calculations and 7.87 ± 0.1 eV on the basis of the charge-transfer experiments.[31−33] It is worth mentioning that we have also performed the ab initio and DFT calculations for predicting the ionization potential of PFA. The B3LPY/6-311+G** calculation yields a value of 61084 cm^{-1} (7.573 eV), which deviates from the measured one by about 2.3%.

3.3. Threshold Ion Spectra. Table 2 lists the vibronic levels of PFA used as intermediate states in the MATI experiments. Figure 5a−f shows the MATI spectra recorded via the 0^0 vibrationless and the $6a^1$, 1^1, 12^1, $6a^11^1$, and $6a^112^1$ vibrational levels in the S_1 state, respectively. Assignments to the observed bands were made mainly on the basis on our ab initio calculations and conformity with the available data of this molecule in the S_0 and S_1 states.[13,14,18,34] The possible assignments to the observed bands in the MATI spectra of PFA are listed in Table 3, along with the calculated frequencies. The Wilson numbering system[35] is used for approximately describing the benzene-like vibrational modes. Some normal vibrations of the PFA ion related to the observed bands in the MATI spectra are illustrated in Figure 6.

3.3.1. MATI Spectra via S_10^0. The MATI spectrum of PFA recorded via the vibrationless level of the S_1 state is shown in Figure 5a. The width of the threshold ion bands is about 10 cm^{-1} (FWHM), which is due to the long-lived ZEKE states and some convolution of molecular rotation in the intermediate state.[28,29] Although this value is about 3 times of that obtained by ZEKE technique for aniline,[36] it is adequate for us to resolve the vibrational features of the PFA ions. The strongest band appears at photon energy of 29 881 cm^{-1} of the ionization laser and corresponds to the production of vibrationless ions. Since MATI spectroscopy involves ionization of molecules in the high Rydberg states by a delayed pulsed electric field, the corresponding ion signal occurs at energy slightly below the ionization threshold. The determination of the ionization threshold should consider the value in the high-energy side of the 0^0 band of the molecular ion.[27,37] It is found that the midpoint of the sharp-rising slope locates at a photon energy of 29 888 cm^{-1} of the ionization laser. This leads to a two-photon energy of 62 540 cm^{-1}. In addition, to obtain accurate ionization energy, one has to take into account the Stark shift for the applied electric field. The lowering of the adiabatic ionization potential (AIE) can be estimated by $4.0F^{1/2}$, where F is the applied pulsed electric field in the unit of V/cm.[38] This suggested that the measured value be increased by 4 cm^{-1}. The field-corrected adiabatic ionization energies obtained by investigating the 0^0 bands in Figure 5a−f are listed in Table 4. Therefore, the AIE determined by the MATI experiments is 62 543 ± 4 cm^{-1}, which is in very good agreement with the value determined by the 2C-R2PI spectroscopy, presented in the previous section.

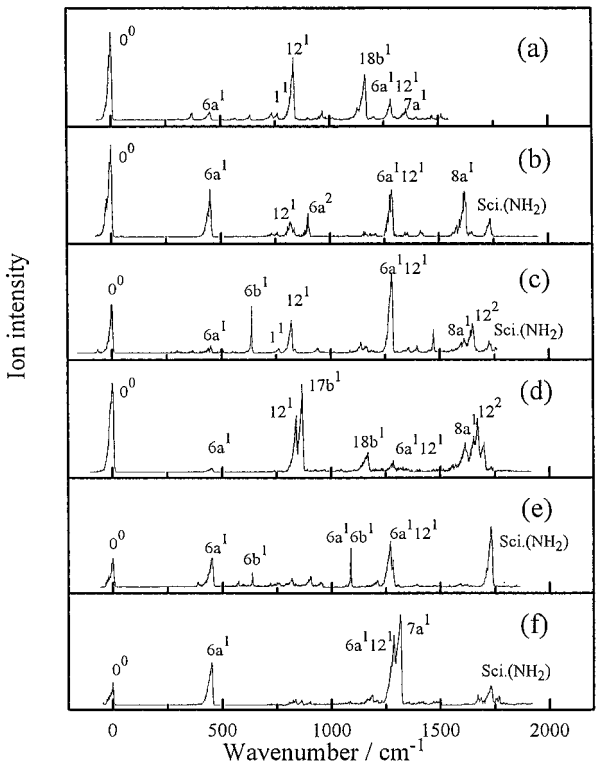

Figure 5. Threshold ion spectra of *p*-fluoroaniline recorded by MATI method via the (a) S_10^0, (b) S_16a^1, (c) S_11^1, (d) S_112^1, (e) $S_16a^11^1$, and (f) $S_16a^112^1$ intermediate states.

The intense band shifted from the 0^0 band by 836 cm^{-1} is assigned to the in-plane ring deformation 12^1 vibration of the PFA cation. The corresponding value of this vibration in the S_1 state has been reported to be 829 cm^{-1}.[13,14,17,18] The other 968 and 1165 cm^{-1} bands are assigned to $18a^1$ and $18b^1$, which are related to the in-plane ring CH bending vibration. The bands corresponding to the in-plane ring deformation $6a^1$ and $6b^1$ and the breathing 1^1 vibrations appear at 452, 634, and 763 cm^{-1}, respectively. The combination band of the $6a^112^1$ motion shows up at 1283 cm^{-1}. It is interesting to note that the substituent-sensitive in-plane CN bending 15^1, CN stretching 13^1, and CF stretching $7a^1$ vibrations are also clearly seen at 371, 1471, and 1352 cm^{-1}, respectively. The 1512 cm^{-1} band is assigned as the $19b^1$ mode, which is related to the in-plane ring CC stretching vibration. A weak band, which appears at 737 cm^{-1}, is tentatively assigned to the NH_2 wagging (inversion) motion.

3.3.2. MATI Spectra via S_16a^1. Figure 5b displays the MATI spectrum of PFA obtained by ionizing through the $6a^1$ vibrational level (33 086 cm^{-1}) in the S_1 state. Pronounced bands at 451 and 901 cm^{-1} are assigned to the fundamental and the

TABLE 3: Observed Bands (in cm^{-1}) in the Threshold Ion Spectra of *p*-Fluoroaniline and Assignments

intermediate level in the S_1 state							
0^0	$6a^1$	1^1	12^1	$6a^11^1$	$6a^112^1$	calcd[a]	assignment[b] and approx description
371				388		354	15^1 X-sens β(CN)
452	451	451	449	455	450	455	$6a^1$ ring β(CCC)
		502				502	$16b^1$ ring γ(CCC)
634		638		637		626	$6b^1$ ring β(CCC)
737	735					748	amino γ(NH) (wagging)
763	760	761				772	1^1 breathing
836	819	820	841	818	835	826	12^1 ring β(CCC)
			867			853	$17b^1$ ring γ(CH)
	901			903	903		$6a^2$ ring β(CCC)
		939		951		969	5^1 ring γ(CH)
968						1010	$18a^1$ ring β(CH)
				1089			$6a^16b^1$ ring β(CCC)
1165		1138	1170		1188	1164	$18b^1$ ring β(CH)
				1215			$6a^11^1$ ring β(CCC)
1283	1285	1282	1285	1271	1286		$6a^112^1$ ring β(CCC)
1352	1356	1358			1314	1342	$7a^1$ X-sens ν(CF)
	1417	1396		1391	1423	1407	3^1 ring β(CH)
1471		1472			1494	1443	13^1 X-sen. ν(CN)
1512			1504			1487	$19b^1$ ring ν(CC)
	1617	1612	1616	1593		1628	$8a^1$ ring ν(CC)
		1650	1672		1671		12^2 ring β(CCC)
	1732	1726		1731	1728	1757	amino β(NH) (scissoring)

[a] At UHF/6-31+G* level of calculations. [b] X-sens, substituent-sensitive; ν, stretching; β, in-plane bending; γ, out-of-plane bending.

TABLE 4: Experimental and Calculated Ionization Energies of *p*-Fluoroaniline

vibronic level for the MATI expts	IE (cm^{-1})
0^0	62 544
$6a^1$	62 544
1^1	62 545
12^1	62 545
$6a^11^1$	62 539
$6a^112^1$	62 541

computational method	IE (cm^{-1})	dev (%)
HF/6-311+G**	51 421	−17.8
MP2/6-31+G*	65 948	5.4
B3PW91/6-31+G*	60 567	−3.2
B3PW91/6-311+G**	61 142	−2.2
B3LYP/6-31+G*	60 469	−3.3
B3LYP/6-311+G**	61 084	−2.3

progression of the in-plane ring deformation mode 6a of the PFA ion. The other two ring deformation modes 1 and 12 appear at 760 and 819 cm^{-1}, respectively. The strong band at 1285 cm^{-1} is then due to the combination mode $6a^112^1$. The band at 1417 cm^{-1} corresponds to the in-plane ring CH bending vibration 3^1, whereas that at 1617 cm^{-1} is related to the CC stretching vibration $8a^1$. The CF stretching vibration occurs at 1356 cm^{-1}, and the scissoring vibration of the NH_2 group appears at 1732 cm^{-1}. The weak band at 735 cm^{-1} corresponds to the NH_2 wagging motion. Many of these modes are also observed in the MATI spectra recorded via other intermediate vibronic states.

3.3.3. MATI Spectra via S_11^1. The MATI spectrum of PFA obtained by ionizing through the S_11^1 vibronic level (33426 cm^{-1}) is shown in Figure 5c. Weak bands at 451 and 761 cm^{-1} are assigned to the ring deformation $6a^1$ and breathing motion 1^1, respectively. This indicates that the transition from the electronically excited S_1 state to the ionic ground state is Franck−Condon unfavorable along these normal coordinates. Vibrations corresponding to the in-plane CCC bending modes 12^1 and 12^2 are observed at 820 and 1650 cm^{-1}, respectively. The noticeable band appearing at 1282 cm^{-1} is related to the coupled motion involving 6a and 12 modes.

The weak band at 502 cm^{-1} is assigned to the out-of-plane ring vibration $16b^1$. A slightly narrower band shows up at 638 cm^{-1}, which corresponds to the frequencies of the 6b vibration of the ion. We did check the experimental conditions for eliminating the possibility of the direct ions resulting from the R2PI processes. However, the reason for the narrowness of this MATI band still remains unclear. The out-of-plane CH bending vibration 5^1 appears 939 cm^{-1}, whereas the in-plane CH bending vibrations 18^1 and 3^1 occur at 1138 and 1396 cm^{-1}, respectively. While the 1358, 1472, and 1612 cm^{-1} bands are assigned to the in-plane CF, CN, and CC stretching vibrations, respectively, the 1726 cm^{-1} band is assigned to the amino scissoring motion.

3.3.4. MATI Spectra via S_112^1. Figure 5d shows the MATI spectrum of PFA obtained by ionizing through the S_112^1 vibronic level (33 481 cm^{-1}). Active in-plane deformation vibrations involving patterns 6a and 12 appear at 449, 841, 1285, and 1672 cm^{-1}, which are assigned as $6a^1$, 12^1, $6a^112^1$, and 12^2, respectively. Pronounced bands shifted from the 0^0 band by 867 and 1170 cm^{-1} correspond to the out-of-plane ring CH and the in-plane ring CH bending vibrations $17b^1$ and $18b^1$ of the PFA ion, respectively.

It is interesting to note that bands related to the substituent-sensitive and CH bending vibrations are absent in this MATI spectrum. This implies that the transition from this intermediate vibronic state to those vibrational levels of the ionic ground state is Franck−Condon limited. However, the in-plane ring CC stretching vibrations $19b^1$ and $8a^1$ are observed at 1504 and 1616 cm^{-1}, respectively.

3.3.5. MATI Spectra via $S_16a^11^1$. It was found that the combination bands $6a_0^1\,1_0^1$ and $6a_0^1\,12_0^1$ are quite pronounced in the one-color R2PI spectrum.[14,18] Thus, they were chosen as intermediate levels for the present MATI experiments. The threshold ion spectrum of PFA recorded by ionizing through the $6a^11^1$ level (33 858 cm^{-1}) in the S_1 state is shown in Figure 5e. It is interesting to note that the most intense band (1731 cm^{-1}) is related to the amino scissoring motion. All noticeable bands observed are related to the inplane ring deformation vibrations. The 455, 637, 818, 903, 1089, 1215, and 1271 cm^{-1} bands are assigned to the $6a^1$, $6b^1$, 12^1, $6a^2$, $6a^16b^1$, $6a^11^1$, and $6a^112^1$ vibrations of the PFA ion, respectively. The substituent-

TABLE 5: Calculated Structure Parameters of *p*-Fluoroaniline at RHF/6-31+G*, CIS/6-31+G*, and UHF/6-31+G* Levels of Calculations for the S_0, S_1, and Ionic States

	S_0	S_1	ionic
	Bond Lengths (Å)		
C_1-C_2	1.392	1.433	1.439
C_2-C_3	1.386	1.364	1.372
C_3-C_4	1.377	1.394	1.407
C_1-N_7	1.402	1.314	1.309
C_4-F	1.339	1.310	1.307
C−H	1.075	1.073	1.074
N−H	0.998	1.006	1.002
$C_1\cdots C_4$	2.771	2.755	2.765
	Bond Angles (deg)		
$\angle C_6C_1C_2$	118.5	119.0	120.0
$\angle C_1C_2C_3$	120.9	120.1	119.5
$\angle C_2C_3C_4$	119.1	118.9	119.1
$\angle C_3C_4C_5$	121.4	123.1	122.8
∠FCC	119.3	118.5	118.6
∠HNH	110.0	116.9	116.4

sensitive in-plane CN bending 15^1 appears at 388 cm^{-1}. Weak bands at 951, 1391, and 1593 cm^{-1} correspond to 5^1, 3^1, and $8a^1$ ring vibrations, as listed in Table 3.

3.3.6. MATI Spectra via $S_1 6a^1 12^1$. Figure 5f shows the MATI spectrum of PFA obtained by ionizing through the $6a^1$-12^1 vibronic level (33 914 cm^{-1}). The pronounced bands at 450 and 1314 cm^{-1} are assigned to the ring-deformation $6a^1$ and substituent-sensitive CF stretching $7a^1$ vibrations, whereas the 1286 cm^{-1} band is due to the coupled motion $6a^1 12^1$ vibration. The band related to the NH_2 scissoring motion is seen at 1728 cm^{-1}. Weak bands at 835, 903, and 1671 cm^{-1} are assigned to the 12^1, $6a^2$, and 12^2 vibrations of the PFA ion, respectively. The in-plane ring CH bending vibrational modes $18b^1$ and 3^1 are observed at 1188 and 1423 cm^{-1}, whereas the substituent-sensitive CN stretching vibration 13^1 is seen at 1494 cm^{-1}.

4. Discussion

4.1. Molecular Structure. PFA in the ground electronic state, $S_0(^1A_1)$, is known to have a nonplanar structure with the hydrogen atoms of the amino group bent out of the aromatic plane by 46°.[10] When it is excited to the $S_1(^1B_2)$ state, this bending angle vanishes as the hydrogen move to the plane of the aromatic ring.[11,12] The delocalization of the lone-paired electrons of the amino group over the aromatic ring causes the molecule in the S_1 state to have a planar structure. Although no experimental data are available, a similar planar structure due to electron delocalization might be expected for PFA in the cationic ground state.

The optimized geometry parameters of PFA in the S_0, S_1, and cationic ground states predicted by using the RHF, CIS, and UHF methods, respectively, with the 6- 31+G* basis set are listed in Table 5. Although the HF/6-31G* calculations (not listed) give a correct prediction for the S_0 state, the CIS/6-31G* calculations do not correctly predict the angle between the ring and the NH_2 planes (referred to as the γ angle) and other parameters for PFA in the S_1 states. Since diffuse functions allow orbitals to occupy a large region of space, they become important for calculations involving molecules with lone-paired electrons in the electronically excited and the ionic states.[39] It was found that the RHF/6-31+G* and the CIS/6-31+G* calculations successfully predict the optimized geometry parameters which include the γ angle, dipole moment, and rotational constants for PFA in the S_0 and S_1 states, respectively.[13] Therefore, the UHF/6-31+G* calculation was performed for predicting the structure of PFA in the cationic ground state. The calculated results show that the neutral $S_0(^1A_1)$ state has a $(a')^2(a'')^2(a')^2$ configuration, whereas the cationic ground state, $^2B_1$, has a $(a_1)^2(b_2)^2(b_1)^1$ configuration. The transition from the neutral to the ionic state corresponds to the removal of one of the lone-paired electrons of the nitrogen. The remaining nonbounded electron on the nitrogen conjugates with one of the π electrons on the ring forming a C=N double bond and causing the PFA ion to be planar. A similar finding has been reported for aniline.[36,40]

4.2. Ionization Energy. Ionization of a molecule by photoionization is governed by the Franck−Condon principle. Thus, when the equilibrium geometries of an ion and its corresponding neutral species are closely similar, the energy dependence of the onset of ionization will be a sharp step function. Spectroscopic studies using short-pulse lasers with well-defined photon energy can provide highly accurate ionization energy values. As shown in Figure 4, a sharp step appears at a two-photon energy of about 62 550 cm^{-1} in the 2C-R2PI spectrum. This result also indicates that the geometry of PFA cation is quite similar to that of the neutral species in the S_1 state. In a different approach, highly accurate determination of ionization energy was achieved by the detection of the threshold ions. Table 4 lists the ionization energy determined by analysis of the threshold ion spectra shown in Figure 5a−f. The mean value of the AIE is 62 543 cm^{-1} on the basis of the MATI experiments, which is in very good agreement with that measured by using the 2C-R2PI method.

Recently, Curtiss et al.[41] pointed out that the ionization potentials could be computed by using the Gaussian-2 (G2) and density functional theories to an accuracy of an absolute deviation of about 0.06 and 0.18 eV, respectively, for a set of 146 molecules. In order to provide a comparison with the present experimental results, we have performed the HF, MP2, and DFT calculations. The computed ionization energies were obtained at the geometries optimized at the RHF/6-31+G* and UHF/6-31+G* levels of theory for the S_0 and ionic states, respectively. As shown in Table 4, the HF/6-311+G** method predicts an ionization energy of about 17.8% lower than the measured value. When the electron correlation is taken into consideration for the energy calculation, the MP2/6-31+G* procedure leads to an overestimated value of 5.4%. Although the G-2 calculations may provide more accurate results, they are quite costly for a medium size molecule like PFA. The density functional methods require about the same amount of computation resources as HF theory, but they account for the instantaneous interactions of pairs of electrons with opposite spin. It was found that both the Becke three-parameter functional with the PW91 correlation functional (B3PW91) and the hybrid B3LYP density functional methods improved the deviation to 3.2%. When a larger basis set is used, the B3PW91/6-311+G** and the B3LYP/6-311+G** calculations underestimate the ionization energy by only 2.2%. These findings are consistent with those reported by Curtiss et al.[41]

It was found that the presently determined ionization energy of PFA is greater than that of aniline (62 271 cm^{-1})[36] by 283 cm^{-1}. As shown in Table 5, the bond lengths of C−F and C−N in the ionic state are shorter than the corresponding ones in the ground state. This suggests that the delocalization of the lone-paired electrons of the nitrogen atom to the aromatic ring also enhances the covalence character of the C−F bond. As mentioned previously, the ionization of FPA as well as aniline corresponds to the removal of one of the lone-paired electrons of nitrogen. The presence of the F atom in the para position of

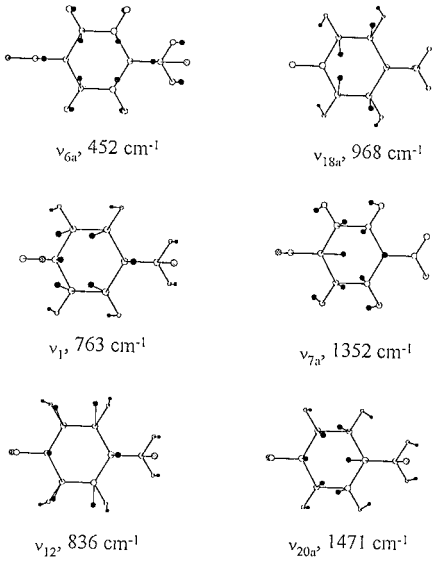

Figure 6. Some normal vibrations related to the observed bands in the threshold ion spectra of *p*-fluoroaniline.

the ring of PFA somewhat prohibits this electronic transition, leading to a higher ionization potential.

4.3. Vibrations. PFA has 36 normal vibrations, which include 30 benzene-like and 6 amino modes. Calculated results show that the planar PFA cation has the C_{2v} symmetry with $13A_1 + 12B_2 + 4A_2 + 7B_1$ normal vibrations. The observed band intensity in the threshold ion spectra is related to the oscillator strength corresponding to the $S_1 \leftarrow S_0$ transition, the transition cross section from the S_1 state to the Rydberg state, and the pulsed field ionization efficiency. Analysis of the band intensity is beyond the scope of the present work. Here, we only discuss the vibrations, which are related to the observed bands in the threshold ion spectra.

Most of the observed bands in the threshold ion spectra correspond to the in-plane vibrations, as listed in Table 3. Among the totally symmetric modes, 6a and 12 represent the in-plane ring deformation, whereas mode 1 is the ring breathing vibration, as seen in Figure 6. The vibrational frequencies of modes 6a, 1, and 12 of PFA ion were measured to be 452, 763, and 836 cm^{-1}, whereas the corresponding ones of aniline ion were reported to be 522, 814, and 984 cm^{-1}, respectively.[36] Since the F atom has a very large electron negativity, it can withdraw electrons from the ring. The present finding indicates that the interaction between the F atom and the ring has reduced the electron density in the phenyl ring of the PFA ion. For the neutral PFA in the S_1 state, the frequencies of modes 6a, 1, and 12 are 434, 744, and 829 cm^{-1}, respectively.[13,14,18,34] As shown in Table 5, the structure parameters of the PFA in the S_1 and ionic states are quite close to each others. Thus, frequency of each normal vibration of the ion is expected to be close to that of the corresponding neutral in the S_1 state. Since the vibrational patterns are similar, the progression and combination bands involving these modes may appear in the spectra of the PFA ion. These bands include $6a^2$, 12^2, $6a^11_1$, and $6a^112^1$, as shown in Table 3.

The in-plane substituent-sensitive CN bending vibration 15^1 of the PFA ion is observed at 371 cm^{-1}. The frequency of this mode for aniline ion has been reported to be 390 cm^{-1}.[36] Thus, the strength of the CN bond may be slightly reduced by the F atom in the para position of the ring. The CF ($7a^1$) and CN (13^1) stretching vibrations appear at 1352 and 1471 cm^{-1}, respectively, in the threshold ion spectra. These measured values match very well with those of calculated ones obtained at the UHF/6-31+G* level. The results also show that the CN bond is stronger than the CF bond. The frequencies of the corresponding modes 7a and 13 have been reported to be 1229 and 1278 cm^{-1}, respectively, for PFA in the ground state.[34] These findings are in good agreement with the result of the investigation on the bond lengths, discussed in the previous section.

Only a few out-of-plane vibrations were observed in the ion spectra of PFA. Mode 16b is an out-of-plane ring deformation, whereas modes 17b and 5 are the CH bending vibrations. The respective frequencies of modes 16b, 17b, and 5 are found at 502, 867, and 939 cm^{-1} for the ion, whereas the corresponding values are 512, 828, and 916 cm^{-1} for the neutral in the ground state. The deviation in the vibrational frequency of these out-of-plane vibrations may result from the change in the density of the π-electron clouds in the phenyl ring upon ionization.

The wagging vibration of the amino group is observed at 737 and 735 cm^{-1} in the threshold ion spectra which are obtained by exciting the PFA molecule via the vibrationless and the $6a^1$ levels in the S_1 state. The corresponding frequency of this amino vibration in and S_1 state has been reported to be 748 cm^{-1}.[13,14,18,34] The reduction in the frequency of this mode indicates that the CN bond of PFA in the ionic state is slightly stronger than that in S_1 state. This observation is consistent with the predicted shorter CN bond length of the PFA ion, as shown in Table 5. In addition, the NH_2 scissoring motion becomes active when PFA is excited via the $6a^1$, 1^1, $6a^11^1$, and $6a^112^1$ levels of the S_1 state, as seen in Figure 5. Since the transition from the neutral to the cationic ground state corresponds to the removal of one of the lone-paired electrons of nitrogen, the observation of the NH_2 vibration implies a great change in the electron density around the nitrogen.

5. Conclusion

Ionic properties of PFA have been studied by using both the MATI and 2C-R2PI spectroscopy. The adiabatic ionization energy of this molecule determined by the former method is 62 543 ± 4 cm^{-1}, whereas that determined by the latter one is 62 550 ± 7 cm^{-1}. In addition, the vibrations of the PFA in the cationic ground state are observed in the threshold ion spectra recorded via the vibrationless 0^0 and the $6a^1$, 1^1, 12^1, $6a^11^1$, and $6a^112^1$ vibrational levels in the S_1 state. The results show that most of the active vibrations of the PFA ion mainly involve in-plane vibration. All these experimental data are presented for the first time for this molecular system.

In order to justify the applicability of our coaxial type molecular beam TOF mass spectrometer for the MATI experiments, detailed studies on the molecular beam containing Rydberg neutrals, spatial separation between the Rydberg neutrals and direct ions were conducted. The most probable velocity of the 0.2% PFA beam seeded in 2.3 bar of helium was measured to be 1400 m s^{-1} by the threshold ionization method with variable delayed electric field. With the known spacings in our ion optics components, the spatial separation between the Rydberg neutrals and direct ions was estimated to be 0.9 mm under normal experimental conditions. This spatial separation will vary with the magnitude of the applied pulsed field in the ion optics elements. In addition, we demonstrated that judicious control on the magnitude and delay time of the separation and extraction pulsed electric fields could yield a clean signal of threshold ions in a coaxial type TOF mass spectrometer. The above-detailed procedures warrant the success of the MATI experiments.

We have also performed computations for the prediction of the ionization energy of PFA, and the structure and vibrational

frequencies of the PFA ion. The B3PW91/6-311+G** and the B3LYP/6-311+G** density functional calculations with the optimized structure at the HF/6-31+G* level underestimate the ionization potential of PFA by about 2.2%, which corresponds to an absolute deviation of 0.18 eV. The calculated frequencies at the UHF/6-31+G* level are in very good agreement with the measured ones in the threshold ion spectra. The results from experimental and theoretical approaches help to gain more insights into the ionic properties of PFA.

Acknowledgment. We thank Professor H. J. Neusser for his helpful suggestions concerning the MATI experimental setup. This work was supported by the National Science Council (Grant No. NSC-89-2113-M-001-024).

References and Notes

(1) Müller-Dethlefs, K.; Sander, M.; Schlag, E. W. *Chem. Phys. Lett.* **1984**, *112*, 291.
(2) Chewter, L. A.; Sander, M.; Müller-Dethlefs, K.; Schlag, E. W. *J Chem. Phys.* **1987**, *86*, 4737.
(3) Held, A.; Schlag, E. W. *Acc. Chem. Res.* **1998**, *31*, 467.
(4) Zhu, L.; Johnson, P. M. *J. Chem. Phys.* **1991**, *94*, 5769.
(5) Willey, K. F.; Yeh, C. S.; Duncan, M. A. *Chem. Phys. Lett.* **1993**, *211*, 156.
(6) Zhang, X.; Pitts, J. D.; Nadarajah, R.; Knee, J. L. *J. Chem. Phys.* **1997**, *107*, 8239.
(7) Braun, J. E.; Grebner, Th. L.; Neusser, H. J. *J. Phys. Chem.* **1998**, *102*, 3273.
(8) Lembach, G.; Brutschy, B. *J. Phys. Chem.* **1998**, *102*, 6068.
(9) Martin, J. D. D.; Hepburn, J. W. *J. Chem. Phys.* **1998**, *109*, 8139.
(10) Hastie, A.; Lister, D. G.; McNeil, R. L.; Tyler, J. K. *J. Chem. Soc., Chem. Commun.* **1970**, 108.
(11) Thakur, S. N.; Tiwari, S. K.; Rai, D. K. *J. Mol. Struct.* **1970**, *5*, 309.
(12) Huang, K. T.; Lombardi, J. R. *J. Chem. Phys. Chem.* **1969**, *51*, 1228.
(13) Tzeng, W. B.; Narayanan, K.; Hsieh, C. Y.; Tung, C. C. *J. Chem. Soc., Faraday Trans.* **1997**, *93*, 2981.
(14) Tzeng, W. B.; Narayanan, K.; Hsieh, C. Y.; Tung, C. C. *Asian J. Spectrosc.* **1997**, *1*, 45.
(15) Shashidhar, M. A.; Rao, K. S.; Jayadevappa, E. S. *Spectrochim. Acta A* **1970**, *26*, 2373.
(16) Kydd, R. A.; Krueger, P. J. *J. Chem. Phys.* **1978**, *69*, 827.
(17) Gordon, R. D.; Clark, D.; Crawley, J.; Mitchell, R. *Spectrochim. Acta A* **1984**, *40*, 657.
(18) Tembreull, R.; Dunn, T. M.; Lubman, D. M. *Spectrochim. Acta A* **1986**, *42*, 899.
(19) Wang, C. R. C.; Hsu, C. C.; Liu, W. Y.; Tsai, W. C.; Tzeng, W. B. *Rev. Sci. Instrum.* **1994**, *65*, 2776.
(20) Tzeng, W. B.; Narayanan, K.; Chang, G. C.; Tsai, W. C.; Ho, J. J. *J. Phys. Chem.* **1996**, *100*, 15340.
(21) Lin, S. H.; Fujimura, Y.; Neusser, H. J.; Schlag, E. W. *Multiphoton Spectroscopy of Molecules*; Academic Press: London, 1984; pp 89−92.
(22) *Gaussian 94*, Revision E.2; Frisch, M. J.; Trucks, G. W.; Schlegel, H. B.; Gill, P. M. W.; Johnson, B. G.; Robb, M. A.; Cheeseman, J. R.; Keith, T.; Petersson, G. A.; Montgomery, J. A.; Raghavachari, K.; Al-Laham, M. A.; Zakrzewski, V. G.; Ortiz, J. V.; Foresman, J. B.; Cioslowski, J.; Stefanov, B. B.; Nanayakkara, A.; Challacombe, M.; Peng, C. Y.; Ayala, P. Y.; Chen, W.; Wong, M. W.; Andres, J. L.; Replogle, E. S.; Gomperts, R.; Martin, R. L.; Fox, D. J.; Binkley, J. S.; Defrees, D. J.; Baker, J.; Stewart, J. P.; Head-Gordon, M.; Gonzalez, C.; Pople, J. A. Gaussian, Inc.: Pittsburgh, PA, 1995.
(23) Krause, H.; Neusser, H. J. *J. Chem. Phys.* **1992**, *97*, 5923.
(24) Grebner, Th. L.; Neusser, H. J. *Int. J. Mass Spectrom. Ion Processes* **1996**, *159*, 137.
(25) Held, A.; Selzle, H. L.; Schlag, E. W. *J. Phys. Chem. A* **1997**, *101*, 535.
(26) Merk, F.; Zare, R. N. *J. Chem. Phys.* **1994**, *101*, 3495.
(27) Hsu, C. W.; Lu, K. T.; Evans, M.; Chen, Y. J.; Ng, C. Y.; Heimann, P. *J. Chem. Phys.* **1996**, *105*, 3950.
(28) Lembach, G.; Brutschy, B. *J. Phys. Chem.* **1996**, *100*, 19758.
(29) Jouvet, C.; Dedonder-Lardeux, C.; Martrenchard-Barra, S.; Solgadi, D. *Chem. Phys. Lett.* **1992**, *198*, 419.
(30) Tzeng, W. B.; Yin, H. M.; Leung, W. Y.; Luo, J. Y.; Nourbakhsh, S.; Flesch, G. D.; Ng, C. Y. *J. Chem. Phys.* **1988**, *88*, 1658.
(31) Lias, S. G.; Bartmess, J. E.; Liebman, J. F.; Holmes, J. L.; Levin, R. D.; Mallard, W. G. *J. Phys. Chem. Ref. Data* **1988**, *17*, Supplement No. 1.
(32) Palmer, M. H.; Moyes, W.; Spiers, M.; Ridyard, J. N. A. *J. Mol. Struct.* **1979**, *53*, 235.
(33) Farrell, P. G.; Newton, J. *Tetrahedron Lett.* **1966**, 5517.
(34) Varsanyi, G. *Assignments of Vibrational Spectra of Seven Hundred Benzene Derivatives*; Wiley: New York, 1974.
(35) Wilson, E. B. *Phys. Rev.* **1934**, *45*, 706.
(36) Song, X.; Yang, M.; Davidson, E. R.; Reilly, J. P. *J. Chem. Phys.* **1993**, *99*, 3224.
(37) Boogaarts, M. G. H.; Holleman, I.; Jongma, R. T.; Parker, D. H.; Meijer, G. *J. Phys. Chem. A* **1996**, *104*, 4357.
(38) Chupka, W. A. *J. Chem. Phys.* **1993**, *98*, 4520.
(39) Foresman, J. B.; Frisch, E. *Exploring Chemistry with Electronic Structure Methods*, 2nd ed.; Gaussian Inc.: Pittsburgh, PA, 1996; p 99.
(40) Kim, B.; Weber, P. M. *J. Phys. Chem.* **1995**, *99*, 2583.
(41) Curtiss, L. A.; Redfern, P. C.; Raghavachari, K.; Pople, J. A. *J. Chem. Phys.* **1998**, *109*, 42.